



LAWRENCE  
LIVERMORE  
NATIONAL  
LABORATORY

# Implicit Monte Carlo Radiation Transport Simulations of Four Test Problems

N.A. Gentile

August 3, 2007

Computational Methods in Transport  
Lake Tahoe, CA, United States  
September 9, 2006 through September 14, 2006

## **Disclaimer**

---

This document was prepared as an account of work sponsored by an agency of the United States Government. Neither the United States Government nor the University of California nor any of their employees, makes any warranty, express or implied, or assumes any legal liability or responsibility for the accuracy, completeness, or usefulness of any information, apparatus, product, or process disclosed, or represents that its use would not infringe privately owned rights. Reference herein to any specific commercial product, process, or service by trade name, trademark, manufacturer, or otherwise, does not necessarily constitute or imply its endorsement, recommendation, or favoring by the United States Government or the University of California. The views and opinions of authors expressed herein do not necessarily state or reflect those of the United States Government or the University of California, and shall not be used for advertising or product endorsement purposes.

---

# Implicit Monte Carlo Radiation Transport Simulations of Four Test Problems

N. A. Gentile

University of California  
Lawrence Livermore National Laboratory  
P. O. Box 808  
Livermore, California 94550  
`gentile1@llnl.gov` \*

**Summary.** Radiation transport codes, like almost all codes, are difficult to develop and debug. It is helpful to have small, easy to run test problems with known answers to use in development and debugging. It is also prudent to re-run test problems periodically during development to ensure that previous code capabilities have not been lost. We describe four radiation transport test problems with analytic or approximate analytic answers. These test problems are suitable for use in debugging and testing radiation transport codes. We also give results of simulations of these test problems performed with an Implicit Monte Carlo photonics code.

## 1 The units used for the simulations described in this work

We describe test problems used in the development and debugging of an Implicit Monte Carlo (IMC) radiation transport package used in the KULL [GKR98] and ALEGRA [BM04] inertial confinement fusion codes. (Details of the IMC algorithm can be found in [FC71].) The test problems were run using cgs units, with temperature in keV.

In these units:

- the speed of light  $c = 2.9979 \times 10^{10}$  cm/s
- Boltzmann's constant  $k = 1.6022 \times 10^{-8}$  erg/keV
- Planck's constant  $h = 6.6262 \times 10^{-27}$  erg-s
- The radiation constant (the  $a$  in  $aT^4$ )  $a = 1.3720 \times 10^{14}$  erg/(cm<sup>3</sup> - keV<sup>4</sup>)
- The Stefan-Boltzmann constant  $\sigma_{SB} = ac/4 = 1.0283 \times 10^{24}$  erg/(cm<sup>2</sup> - s - keV<sup>4</sup>).

---

\* This work was performed under the auspices of the U.S. Department of Energy by University of California Lawrence Livermore National Laboratory under contract No. W-7405-ENG-48.

## 2 A gray infinite medium problem with a matter energy source allowing an analytic answer

Here we describe a test problem with no spatial dependence. A source of energy which heats the matter, constant in space and time, acts on a medium with a constant opacity and an equation of state specified so as to linearize the coupled radiation and matter energy equations. The linearized equations have an analytic solution for the matter and radiation energy density. An IMC simulation is compared to the analytic answer.

The time-dependent transport equation for gray photons in the absence of scattering in an infinite medium is [P73]

$$\frac{1}{c} \frac{\partial I}{\partial t} = -\sigma I + \frac{c\sigma a T_m^4}{4\pi}, \quad (1)$$

where  $\sigma$  is the absorption cross section in inverse length units and  $T_m$  is the matter temperature. The transport equation is coupled to the material energy balance equation [P73]

$$\frac{\partial e_m}{\partial t} = \sigma \int I d\Omega - c\sigma a T^4 + \frac{\rho}{4\pi} \frac{d\epsilon}{dt}. \quad (2)$$

Here,  $e_m$  is the matter energy density in units of energy per volume,  $\epsilon$  is the specific energy in units of energy per mass,  $\rho$  is the mass density, and  $c_v$  is the heat capacity in units of energy per mass per temperature. The matter energy source is specified as the time rate of change of specific energy, in units of energy per mass per time.

In this section, we will use the following equation of state (EOS) relating  $e_m$  and  $T_m$ :

$$e_m = \frac{\alpha}{4} T^4, \quad (3)$$

where  $\alpha$  is a constant. This EOS has  $c_v = \alpha T_m^3 / \rho$ .

The radiation energy density is defined as

$$e_r = \frac{1}{c} \int I d\Omega. \quad (4)$$

If we integrate Eqs. 1 and 2 over  $\Omega$ , and employ the EOS described in Eq. 3 and the definition of energy density Eq. 4, we get the following equations for the radiation energy density and matter energy density:

$$\frac{\partial e_r}{\partial t} = -c\sigma e_r + c\sigma \frac{4a}{\alpha} e_m \quad (5)$$

$$\frac{\partial e_m}{\partial t} = c\sigma e_r - c\sigma \frac{4a}{\alpha} e_m + \rho \frac{d\epsilon}{dt}. \quad (6)$$

With constant  $\rho$  and  $\sigma$ , these coupled ordinary differential equations are linear. The solution can be found in, for example, [BD77]. It is expressed most conveniently in terms of the following definitions:

$$\begin{aligned} \tau &\equiv c\sigma t \\ \beta &\equiv \frac{4a}{\alpha} \end{aligned}$$

$$\begin{aligned}
\lambda &\equiv -(1 + \beta) \\
e_{total}(t) &\equiv e_r(t) + e_m(t) \\
&= e_r(0) + e_m(0) + \rho \frac{d\epsilon}{dt} \\
K_0 &\equiv - \left[ \frac{\beta \rho}{c\sigma\lambda^2} \frac{d\epsilon}{dt} + \frac{\beta e_{total}(0)}{\lambda} \right] \\
K_\lambda &\equiv e_r(0) - K_0.
\end{aligned} \tag{7}$$

In terms of these definitions, we get:

$$e_r(\tau) = K_0 - \frac{\beta}{c\sigma\lambda} \rho \frac{d\epsilon}{dt} \tau + K_\lambda e^{\lambda\tau} \tag{8}$$

$$e_m(\tau) = e_{total}(\tau) - e_r(\tau) = e_{total}(0) + \rho \frac{d\epsilon}{dt} \frac{\tau}{c\sigma}. \tag{9}$$

The IMC simulation of this test problem used the following parameters:

- $\alpha = 4.0a = 5.4881 \times 10^{14} \text{ erg}/(\text{cm}^3 - \text{keV}^4)$
- $\sigma = 1.0 \text{ cm}^{-1}$
- $d\epsilon/dt = 1.0 \times 10^{24} \text{ erg}/(\text{g-s})$
- $T_m(0) = 0.1 \text{ keV}$ .

The mesh was a unit cube with sides of 1 cm and reflecting boundary conditions on all 6 faces. The simulation used  $\Delta t = 1.0 \times 10^{-12} \text{ s}$ , which is the equivalent of  $\Delta\tau = 2.9979 \times 10^{-2}$ . The simulation was run for 1000 time steps with a constant  $\Delta t$ , to a time of  $1.0 \times 10^{-9} \text{ s}$  ( $\tau = 29.979$ ).

The results of the IMC simulation compared to the analytic answer are shown in Fig. 1. The IMC simulation used  $10^4$  particles and took approximately 1 minute on a Pentium 4 processor. The radiation and matter temperature are derived from the analytic expressions for the matter energy density given by Eqs. 8 and 9:  $T_m = \sqrt[4]{4e_m/\alpha}$  and  $T_r = \sqrt[4]{e_r/a}$ . The IMC results for both  $T_r$  and  $T_m$  match the analytic results very well.

### 3 A cube with a face source allowing an approximate analytic answer

A problem similar to the preceding one can be obtained by replacing the matter energy source with a constant temperature source on one face. (The other 5 faces remain reflecting boundaries.) This problem is no longer an infinite medium problem. However, if we ignore the spatial variation in matter and radiation energy density in the cube, it can be approximated as an infinite medium problem. This assumption is justified if the light travel time across the cube is short compared to the time scale on which the matter and radiation energy densities are changing. In that case,  $T_m$  and  $T_r$  can reach an approximately constant value across the cube.

The radiation energy input per unit area from a temperature face source with temperature  $T_s$  is  $\sigma_{SB}T_s^4$ . If we assume that the absorption opacity  $\sigma$  is large enough that most source photons are absorbed before being reflected out of the cube, then we can approximate the energy leaving the problem through the source face per unit area as  $\sigma_{SB}T_m^4$ .

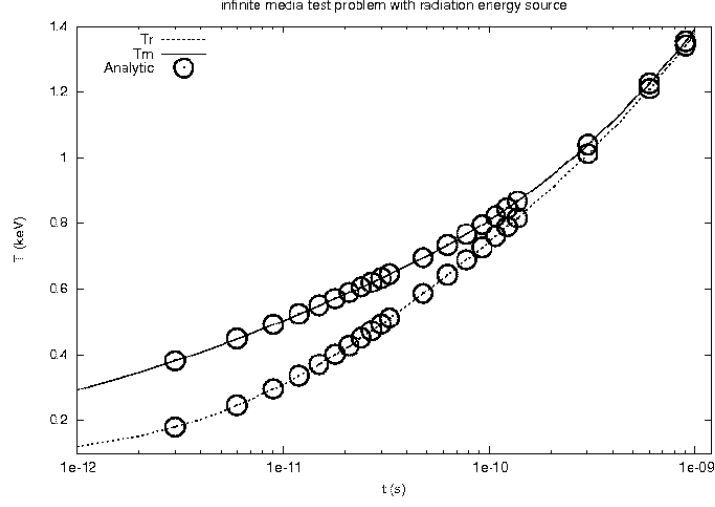


**Fig. 1.** The IMC results for the linearized infinite medium test problem and the analytic answer for the matter and radiation temperature, derived from the energy density given by Eqs. 8 and 9. Temperature is plotted vs time. The temperature is in units of keV and the time is in units of seconds.

With these assumptions, Eqs. 5 and 6 become

$$\frac{\partial e_r}{\partial t} = -c\sigma e_r + c\sigma \frac{4a}{\alpha} e_m + \frac{1}{4} \frac{ac}{L} [T_s^4 - e_m/(\alpha/4)] \quad (10)$$

$$\frac{\partial e_m}{\partial t} = c\sigma e_r - c\sigma \frac{4a}{\alpha} e_m. \quad (11)$$

Here  $L$  is the length of the cube.

These coupled linear ODEs can be solved by the techniques found in, for example, [BD77]. In order to cast the solution into a relatively easily useable form, we need to make several definitions. We start by noting that the asymptotic solution as  $t \rightarrow \infty$  on physical grounds must satisfy  $T_m = T_r = T_s$ . Then we make the following definitions:

$$\begin{aligned} \hat{e}_r(t) &\equiv \frac{e_r(t)}{e_r(t \rightarrow \infty)} = \frac{e_r(t)}{aT_s^4} \\ \hat{e}_m(t) &\equiv \frac{e_m(t)}{e_m(t \rightarrow \infty)} = \frac{e_m(t)}{\alpha/4T_s^4} \\ \tau &\equiv c\sigma t \\ \beta &\equiv \frac{4a}{\alpha} \\ \lambda_{\pm} &\equiv \frac{1}{2} \left[ -(1 + \beta) \pm \sqrt{(1 + \beta)^2 - \frac{\beta}{\sigma L}} \right] \end{aligned} \quad (12)$$

(Note that  $\lambda$  is real if  $\sigma L \gg \beta$ . This is consistent with the assumption that  $\sigma$  was large enough that most of the entering source photons are absorbed.)

Using these definitions, the solutions are

$$\begin{aligned} \hat{e}_r(\tau) &= 1 + C_{r+}e^{\lambda+\tau} + C_{r-}e^{\lambda-\tau} \\ \hat{e}_m(\tau) &= 1 + C_{m+}e^{\lambda+\tau} + C_{m-}e^{\lambda-\tau} \end{aligned} \quad (13)$$

with

$$\begin{aligned} C_{m\pm} &\equiv \frac{C_{r\pm}}{1 + \lambda_{\pm}/\beta} \\ C_{r+} &\equiv \hat{e}_r(0) - 1 - C_{r-} \\ C_{r-} &\equiv \frac{\hat{e}_m(0) - 1 - \frac{\hat{e}_r(0)-1}{1+\lambda_+/\beta}}{\frac{1}{1+\lambda_-/\beta} - \frac{1}{1+\lambda_+/\beta}}. \end{aligned} \quad (14)$$

Results of the IMC simulation are plotted in Fig. 2. The mesh used was a unit cube with a temperature face source on  $z = 0$  and reflecting boundaries on the other faces. The simulation used  $\Delta t = 1.0 \times 10^{-12}$  s, which is the equivalent of  $\Delta\tau = 2.9979 \times 10^{-2}$ . The simulation was run for 1000 time steps with a constant  $\Delta t$ , to a time of  $1.0 \times 10^{-9}$  s ( $\tau = 29.979$ ). The simulation used  $10^4$  particles and took approximately 1 minute on a Pentium 4 processor. The matter temperature calculated by IMC agrees reasonably well with Eq. 13 at all times. The radiation temperature from the IMC simulation is lower than that derived from Eq. 13 at early times, but begins to agree reasonably well after about  $t = 2.0 \times 10^{-11}$  s.

#### 4 Graziani's spherical multigroup prompt spectrum test problem

Graziani [G07] has developed an analytic solution for a time-dependent multigroup radiation transport test problem in spherical geometry. The test consists of a sphere, held at a fixed temperature  $T_s$ , embedded in an infinite medium, the temperature of which is held fixed at  $T_c$ . The embedded sphere begins radiating into the surrounding medium at  $t = 0$ . The medium has a multigroup opacity, which is constant in time because the temperature is held fixed. As radiation from the embedded sphere passes through the surrounding medium, groups with different opacities are absorbed in varying amounts. The radiation energy density at a given point in the medium some distance from the sphere at time  $t > 0$  is the sum of 2 contributions: a Planckian at  $T_c$  from the local material, and an attenuated Planckian at  $T_s$  from the part of the sphere at a distance less than  $ct$  from the given point. This is illustrated in Fig. 3.

Graziani has constructed an analytic expression for the radiation energy density in each group at a given point in the medium as a function of time. He refers to this as the prompt spectrum because it is the correct expression for the radiation energy density at times that are short compared to the time scale for the medium to change temperature. Graziani has derived analytic expressions for both diffusion and transport. In this paper, we will discuss only the transport solution.

Here we give the analytic expression for the prompt spectrum at a fiducial point  $r$  outside the embedded sphere of radius  $R$  at time  $t$  [G07]. The multigroup absorption opacity is denoted by  $\sigma_\nu$  to indicate that it is a function of the frequency group.

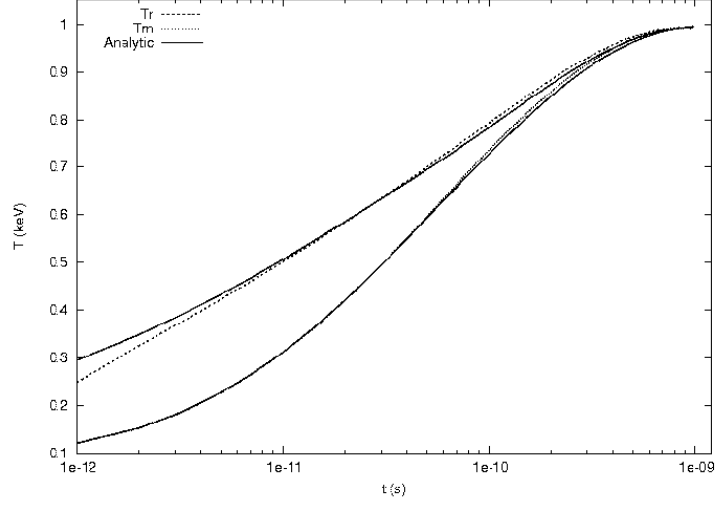


**Fig. 2.** The IMC results for the linearized face source test problem and the approximate analytic answer for the matter and radiation temperature, derived from the energy density given by Eqs. 13 and 14. Temperature is plotted vs time. The temperature is in units of keV and the time is in units of seconds.

$$e_r(r, t, \nu) = B_\nu(T_c) + [B_\nu(T_s) - B_\nu(T_c)]F_\nu(r, t) \quad (15)$$

In this expression,  $e_r$  is the radiation energy density, and  $B_\nu(T)$  is the Planck function,

$$B_\nu(T) = \frac{2h\nu^3/c^2}{\exp(h\nu/kT) - 1}. \quad (16)$$

$F_\nu(r, t)$  is given by

$$F_\nu(r, t) = 0 \quad (17)$$

for  $ct < r - R$ ,

$$\begin{aligned} F_\nu(r, t) = \frac{R}{4r} \left\{ \left[ 1 + \frac{r}{R} - \frac{1}{R\sigma_\nu} \right] e^{-\sigma_\nu(r-R)} \right. \\ \left. + \left[ \frac{1}{R\sigma_\nu} - \frac{R}{ct} \left( \frac{r^2}{R^2} - 1 \right) \right] e^{-\sigma_\nu ct} \right. \\ \left. - R\sigma_\nu \left( \frac{R^2}{R^2} - 1 \right) [E_1(\sigma_\nu(r-R)) - E_1(\sigma_\nu ct)] \right\} \end{aligned} \quad (18)$$

for  $r - R < ct < \sqrt{r^2 - R^2}$ , and

$$F_\nu(r, t) = \frac{R}{4r} \left\{ \left[ 1 + \frac{r}{R} - \frac{1}{R\sigma_\nu} \right] e^{-\sigma_\nu(r-R)} \right.$$



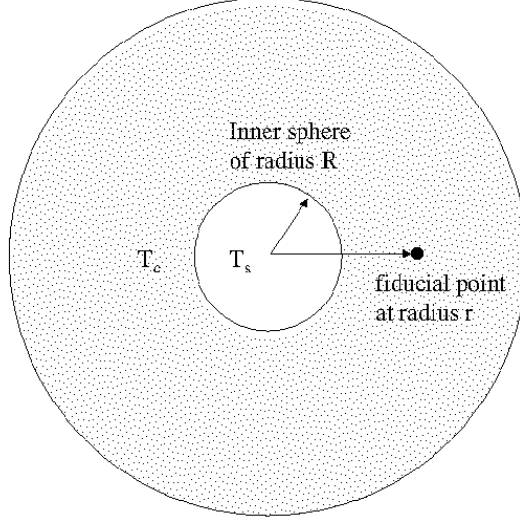


**Fig. 3.** The geometry of the Graziani spherical prompt spectrum problem. An inner sphere of radius  $R$  is embedded in an infinite medium. The temperature of the embedded sphere is held fixed at  $T_s$ . The temperature of the medium outside the sphere is held at  $T_c$ . Photons from the embedded sphere begin to radiate into the medium at  $t = 0$ . The radiation energy density at the fiducial point at radius  $r$  is the sum of a Planckian at  $T_c$  and a time-dependent contribution from the fraction of photons from the source (a Planckian at  $T_s$ ) that make it out to radius  $r$  without being absorbed.

$$\begin{aligned}
 & + \left[ \frac{1}{R\sigma_\nu} - \sqrt{\frac{r^2}{R^2} - 1} \right] e^{-\sigma_\nu \sqrt{r^2 - R^2}} \\
 & - R\sigma_\nu \left( \frac{R^2}{R^2} - 1 \right) \left[ E_1(\sigma_\nu(r - R)) - E_1(\sigma_\nu \sqrt{r^2 - R^2}) \right] \Big\} \quad (19)
 \end{aligned}$$

for  $\sqrt{r^2 - R^2} < ct < \infty$ .

In these expressions for  $F$ ,  $E_1$  is the exponential integral:

$$E_1 = \int_1^\infty \frac{e^{-xt}}{t} dt = \int_x^\infty \frac{e^{-u}}{u} du. \quad (20)$$

See [CTh68] for a rational function approximation, and [PTVF02] for a series approximation.

Details of the IMC simulation follow. The embedded sphere radius  $R$  was taken to be 0.02 cm. The solution is calculated for a fiducial point at radius  $r = 0.04$  cm. The  $T_s = 0.3$  keV and  $T_c = 0.03$  keV. The density of the material is 0.0916 g/cm<sup>3</sup> and is held fixed throughout the simulation. The heat capacity was set to

$10^{50}$  erg/(g-keV). This caused the material temperature to remain constant. Since the density and temperature of the material do not change, the opacity is constant also, and only one value of the opacity for each group is needed for the simulation. (The values given in column 5 in Table 1 can be employed in simulations in order to compare to the analytic answer given in column 4.) The IMC simulation used a tabular opacity calculated for plastic in which some hydrogen atoms were replaced by bromine. This material is frequently used in ICF simulations. Fifty groups were used. The group boundaries were spaced logarithmically between  $3.0 \times 10^{-3}$  keV and 30.0 keV. The opacity of the material at  $T = 0.03$  keV and a density of  $\rho = 0.0916$  g/cm<sup>3</sup> is shown in Fig. 4.

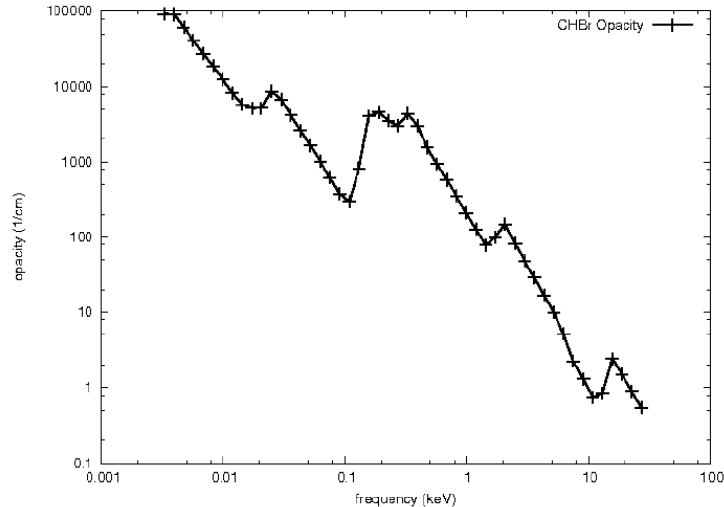


**Fig. 4.** The opacity of brominated plastic used in the Graziani prompt spectrum simulation as a function of frequency. The opacity is in units of 1/cm and the frequency is in units of keV.

The problem was run to a time of  $1.4 \times 10^{-12}$  s using a time step of  $\Delta t = 10^{-13}$  s. (Because the radiation energy density in the IMC algorithm is centered at the half time steps, the answer generated by the IMC simulation corresponds to a time of  $1.35 \times 10^{-12}$  s.)

The analytic solution of this problem is spherical. However, it is not necessary to run a whole sphere, or run the problem in spherical coordinates. It is also not necessary to simulate the inner sphere. It can be replaced by a face temperature source with a temperature of  $T_s$ . The outer boundary of the problem does not have to extend very far past the fiducial point. The outer boundary should have a face temperature source with a temperature of  $T_c$  imposed on it to avoid edge effects.

The IMC simulation was run in Cartesian coordinates on a 3D grid of 11 hexagons. These were stacked in the  $z$  direction. The first zone had the inner face at  $z = 0.02$  cm, the radius of the inner sphere. The center of the 10<sup>th</sup> zone is the fiducial point location at  $z = 0.04$  cm. This requires that  $9.5\Delta z = 0.02$  cm; thus  $\Delta z = 2.10526316 \times 10^{-3}$  cm. The  $x$  and  $y$  coordinates of the nodes of the zone were on lines radiating from  $z = 0$  at a 10 degree angle. Reflecting boundary conditions are imposed on the faces that are not in the  $x$ - $y$  plane. This mesh is pictured in Fig. 5.

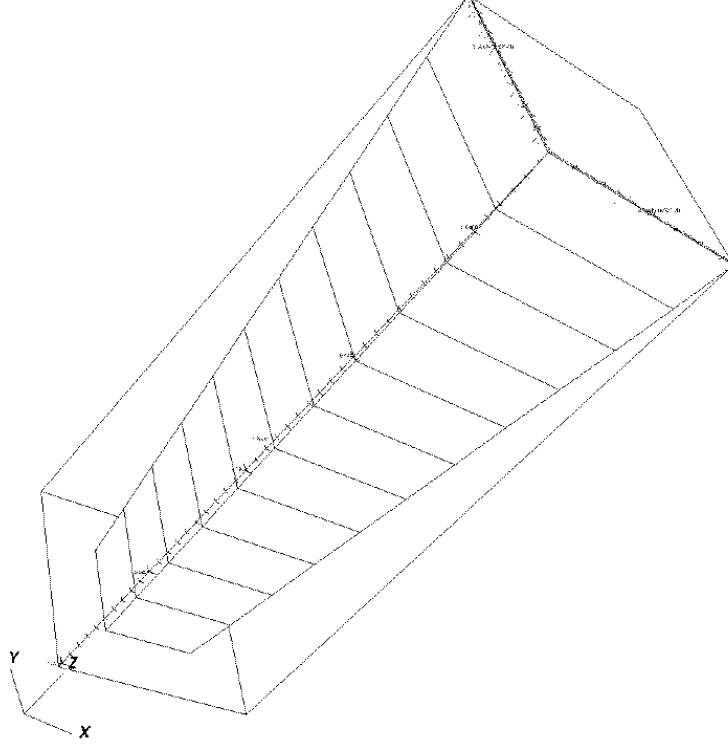


**Fig. 5.** The mesh used in the IMC simulation of the spherical Graziani prompt spectrum problem. The mesh has eleven zones in the  $z$  direction. The innermost zone is at  $z = 0.02$  cm and the outermost is at  $z = 0.043157895$  cm, with  $\Delta z = 2.10526316 \times 10^{-3}$  cm =  $0.02/9.5$  cm. The center of the 10<sup>th</sup> zone is the fiducial point location at  $z = 0.04$  cm.

The results of the simulation, the analytic answer, and the opacity are given for each group in Table 1.

The results of the IMC simulation, and the analytic answer, are shown in Fig. 6. (This is a plot of column 3 and column 4 vs. column 2 of Table 1.) This plot shows the

**Table 1.** Results of the IMC simulation of the Graziani spherical prompt spectrum problem.  $e_r$  is the result of an IMC simulation, and analytic  $e_r$  results from Eqs. 15 and 19, with  $r = 0.04$  cm,  $t = 1.35 \times 10^{-12}$  s, and  $\sigma_\nu$  as given in column 5. The value of  $\nu$  for each group is the rms value of the group bounds, which were logarithmically distributed between  $3.0 \times 10^{-3}$  keV and 30.0 keV. The energy density is in units of erg/(cm<sup>3</sup> – keV) and the opacity is in units of 1/cm.

group	$\nu$	$e_r$	analytic $e_r$	$\sigma_\nu$
0	3.28943e-03	3.60690e+06	6.56128e+06	9.16000e+04
1	3.95477e-03	6.06118e+06	9.37744e+06	9.06781e+04
2	4.75468e-03	1.12608e+07	1.33706e+07	6.08939e+04
3	5.71638e-03	9.30579e+06	1.90091e+07	4.08607e+04
4	6.87260e-03	3.25408e+07	2.69304e+07	2.72149e+04
5	8.26269e-03	3.50625e+07	3.79893e+07	1.86425e+04
6	9.93393e-03	6.14524e+07	5.33093e+07	1.24389e+04
7	1.19432e-02	7.57451e+07	7.43291e+07	8.19288e+03
8	1.43589e-02	1.15741e+08	1.02827e+08	5.79710e+03
9	1.72632e-02	2.20469e+08	1.40887e+08	5.14390e+03
10	2.07549e-02	1.95919e+08	1.90765e+08	5.20350e+03
11	2.49529e-02	2.11776e+08	2.54559e+08	8.69569e+03
12	3.00000e-02	3.48662e+08	3.33604e+08	6.67314e+03
13	3.60679e-02	3.96097e+08	4.27461e+08	4.15912e+03
14	4.33632e-02	4.44384e+08	5.32466e+08	2.62038e+03
15	5.21340e-02	6.73583e+08	6.40012e+08	1.64328e+03
16	6.26789e-02	6.76189e+08	7.35205e+08	1.01613e+03
17	7.53566e-02	7.34447e+08	7.97303e+08	6.19069e+02
18	9.05986e-02	6.17024e+08	8.04394e+08	3.75748e+02
19	1.08923e-01	7.15130e+08	7.43877e+08	2.97349e+02
20	1.30955e-01	5.83979e+08	6.06784e+08	8.21172e+02
21	1.57442e-01	4.41725e+08	4.32675e+08	4.01655e+03
22	1.89287e-01	2.62729e+08	2.59951e+08	4.54828e+03
23	2.27573e-01	1.46260e+08	1.26955e+08	3.50487e+03
24	2.73603e-01	3.47654e+07	4.83345e+07	3.02359e+03
25	3.28943e-01	1.30942e+07	1.36588e+07	4.34203e+03
26	3.95477e-01	3.79204e+06	2.70428e+06	2.98594e+03
27	4.75468e-01	8.89654e+05	3.50392e+05	1.55364e+03
28	5.71638e-01	0.00000e+00	2.74523e-12	9.42213e+02
29	6.87260e-01	0.00000e+00	1.31590e+05	5.76390e+02
30	8.26269e-01	1.40974e+07	1.70905e+07	3.52954e+02
31	9.93393e-01	4.24349e+08	3.95663e+08	2.09882e+02
32	1.19432e+00	2.30338e+09	2.30389e+09	1.26546e+02
33	1.43589e+00	5.60175e+09	5.46696e+09	7.80087e+01
34	1.72632e+00	2.15155e+09	2.16292e+09	9.97421e+01
35	2.07549e+00	3.88801e+08	3.78948e+08	1.48848e+02
36	2.49529e+00	7.93594e+08	7.67169e+08	8.22907e+01
37	3.00000e+00	5.99171e+08	5.58890e+08	4.86915e+01
38	3.60679e+00	2.18511e+08	2.12224e+08	2.91258e+01
39	4.33632e+00	5.48765e+07	4.60720e+07	1.68133e+01
40	5.21340e+00	5.30714e+06	5.53396e+06	9.92194e+00
41	6.26789e+00	1.19953e+06	3.63829e+05	5.18722e+00
42	7.53566e+00	0.00000e+00	1.18769e+04	2.24699e+00
43	9.05986e+00	0.00000e+00	1.68621e+02	1.29604e+00
44	1.08923e+01	0.00000e+00	9.26939e-01	7.46975e-01
45	1.30955e+01	0.00000e+00	1.62634e-03	8.43058e-01
46	1.57442e+01	0.00000e+00	7.11158e-07	2.43746e+00
47	1.89287e+01	0.00000e+00	6.49680e-11	1.50509e+00
48	2.27573e+01	0.00000e+00	8.32408e-16	9.01762e-01
49	2.73603e+01	0.00000e+00	1.00856e-21	5.38182e-01

radiation energy density in  $\text{erg}/(\text{cm}^3 - \text{keV})$  as a function of frequency in keV. The energy density has two maxima. The first, centered around 0.1 keV, is a Planckian formed from emission of the local material at  $T_c = 0.03$  keV. The opacity of the material is very high at frequencies less than 0.5 keV, so almost no photons from the source get to the fiducial point in this range. The second maxima, centered around 1.0 keV, is formed by photons from the source that have passed through the outer material. The Planckian source, at  $T_s = .3$  keV, radiates at a peak frequency of approximately 1 keV. Since the opacity of the material is low for frequencies equal to or greater than 1 keV, higher frequency photons from the source can get to the fiducial point and contribute to the energy density in some of the higher frequency groups.

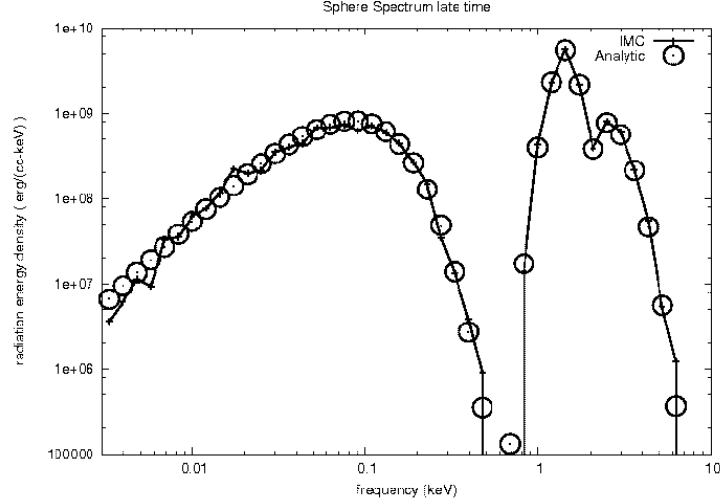


**Fig. 6.** The IMC results for the Graziani prompt spectrum problem and the analytic answer, Eqs. 15 and 19. Radiation energy density is plotted vs. frequency. Values of energy density at frequencies below .5 keV are from the thermal emission at  $T_c$  by the local matter. Values of energy density at frequencies above .5 keV are from higher frequency photons from the source, which have not been fully absorbed. These photons have frequencies at which the brominated plastic opacity has a low opacity and hence a large mean free path. (See Fig. 4.) The energy density is in units of  $\text{erg}/\text{cm}^3 - \text{keV}$  and the frequency is in units of keV.

The IMC simulation used  $8 \times 10^5$  particles and took about 2 minutes on 4 Pentium processors. The simulation answers are in good agreement with the analytic results. Some statistical noise is evident in groups with less energy in them. This is expected, since regions with lower energy density are represented by fewer particles.

## 5 A slab version of Graziani's prompt spectrum test problem

The analytic answer to a slab version of Graziani's test problem can be derived from Eqs. 18 and 19. Define  $d \equiv r - R$ , the distance of the fiducial point from the embedded sphere. Then let both  $r$  and  $R$  grow without bound, while keeping  $d$  fixed. In this limit, the embedded sphere becomes a plane source. The solutions become functions of  $d$ :

$$e_r(r, t, \nu) = B_\nu(T_c) + B_\nu(T_s) - B_\nu(T_c)F_\nu(d, t) \quad (21)$$

with  $F_\nu(d, t)$  given by

$$F_\nu(r, t) = 0, ct < d \quad (22)$$

$$F_\nu(d, t) = \frac{1}{2} \left\{ e^{-\sigma_\nu d} - \frac{d}{ct} e^{-\sigma_\nu ct} - \sigma_\nu d [E_1(\sigma_\nu d) - E_1(\sigma_\nu ct)] \right\} \quad (23)$$

for  $d < ct < \infty$

Since there is always some part of the source plane that is not in causal contact with the fiducial point, there is no steady-state solution for the slab case.

The slab version of Graziani's test problem was simulated using the same material as the spherical version. The same opacities and group structure were used. A face temperature source with a temperature of  $T_s$  is imposed at  $z = 0$ . The outer boundary of the problem had a face temperature source with a temperature of  $T_c$  imposed on it to avoid edge effects.

The mesh used had 11 zones spanning  $[0.0, z = 2.3157895 \times 10^{-2} \text{ cm}]$ . The center of the 10<sup>th</sup> zone is the fiducial point location at  $z = 0.02 \text{ cm}$ , i.e.,  $d = 0.02 \text{ cm}$ . The zones had extent 1 cm in the ignorable  $x$  and  $y$  directions.

As in the spherical case, the simulation was run to a time of  $1.4 \times 10^{-12} \text{ s}$  using a time step of  $\Delta t = 10^{-13} \text{ s}$ , and the answer generated by the IMC simulation corresponds to a time of  $1.35 \times 10^{-12} \text{ s}$ .

The results of the simulation, the analytic answer, and the opacity for the slab case are given for each group in Table 2.

The results of the IMC simulation of the slab problem and the analytic answer, are shown in Fig. 7. (This is a plot of column 3 and column 4 vs. column 2 of Table 2.) This plot shows the radiation energy density in  $\text{erg}/(\text{cm}^3\text{-keV})$  as a function of frequency in keV. As in the sphere case, the energy density has two maxima. The height of the maxima centered near 1 keV is higher in the sphere case, because the plane source emits many more photons toward the fiducial point than a spherical source at the same distance.

Because the source is stronger in the slab case, the IMC simulation used more particles and took slightly longer. The simulation used  $2 \times 10^6$  particles and took about 3 minutes on 4 Pentium processors. As in the sphere case, the simulation answers are in good agreement with the analytic results, and some statistical noise is evident in groups with lower energy density.

**Table 2.** Results of the IMC simulation of the Graziani slab prompt spectrum problem.  $e_r$  is the result of an IMC simulation, and analytic  $e_r$  results from Eqs. 21 and 23, with  $d = 0.02$  cm,  $t = 1.35 \times 10^{-12}$  s, and  $\sigma_\nu$  as given in column 5. The value of  $\nu$  for each group is the rms value of the group bounds, which were logarithmically distributed between  $3.0 \times 10^{-3}$  keV and 30.0 keV. The energy density is in units of erg/(cm<sup>3</sup> – keV) and the opacity is in units of 1/cm.

group	$\nu$	$e_r$	analytic $e_r$	$\sigma$
0	3.28943e-03	0.00000e+00	6.56128e+06	9.16000e+04
1	3.95477e-03	0.00000e+00	9.37744e+06	9.06781e+04
2	4.75468e-03	6.08837e+06	1.33706e+07	6.08939e+04
3	5.71638e-03	2.21914e+07	1.90091e+07	4.08607e+04
4	6.87260e-03	0.00000e+00	2.69304e+07	2.72149e+04
5	8.26269e-03	3.39862e+07	3.79893e+07	1.86425e+04
6	9.93393e-03	9.77224e+07	5.33093e+07	1.24389e+04
7	1.19432e-02	5.35097e+07	7.43291e+07	8.19288e+03
8	1.43589e-02	1.28744e+08	1.02827e+08	5.79710e+03
9	1.72632e-02	9.27517e+07	1.40887e+08	5.14390e+03
10	2.07549e-02	1.57907e+08	1.90765e+08	5.20350e+03
11	2.49529e-02	2.83336e+08	2.54559e+08	8.69569e+03
12	3.00000e-02	3.82734e+08	3.33604e+08	6.67314e+03
13	3.60679e-02	5.08110e+08	4.27461e+08	4.15912e+03
14	4.33632e-02	4.12233e+08	5.32466e+08	2.62038e+03
15	5.21340e-02	4.44628e+08	6.40012e+08	1.64328e+03
16	6.26789e-02	9.17212e+08	7.35205e+08	1.01613e+03
17	7.53566e-02	8.23536e+08	7.97306e+08	6.19069e+02
18	9.05986e-02	6.79309e+08	8.05117e+08	3.75748e+02
19	1.08923e-01	9.75612e+08	7.49915e+08	2.97349e+02
20	1.30955e-01	8.02509e+08	6.06784e+08	8.21172e+02
21	1.57442e-01	3.78322e+08	4.32675e+08	4.01655e+03
22	1.89287e-01	2.77227e+08	2.59951e+08	4.54828e+03
23	2.27573e-01	1.14425e+08	1.26955e+08	3.50487e+03
24	2.73603e-01	5.79367e+07	4.83345e+07	3.02359e+03
25	3.28943e-01	1.37617e+07	1.36588e+07	4.34203e+03
26	3.95477e-01	2.32763e+06	2.70428e+06	2.98594e+03
27	4.75468e-01	0.00000e+00	3.50392e+05	1.55364e+03
28	5.71638e-01	0.00000e+00	2.75095e+04	9.42213e+02
29	6.87260e-01	0.00000e+00	2.85002e+05	5.76390e+02
30	8.26269e-01	3.22636e+07	3.91809e+07	3.52954e+02
31	9.93393e-01	9.34736e+08	9.85459e+08	2.09882e+02
32	1.19432e+00	6.30907e+09	6.33419e+09	1.26546e+02
33	1.43589e+00	1.64366e+10	1.64600e+10	7.80087e+01
34	1.72632e+00	6.11433e+09	6.22834e+09	9.97421e+01
35	2.07549e+00	9.91868e+08	1.00872e+09	1.48848e+02
36	2.49529e+00	2.36965e+09	2.28836e+09	8.22907e+01
37	3.00000e+00	1.77814e+09	1.80809e+09	4.86915e+01
38	3.60679e+00	7.47867e+08	7.26508e+08	2.91258e+01
39	4.33632e+00	1.37272e+08	1.64067e+08	1.68133e+01
40	5.21340e+00	1.77538e+07	2.01749e+07	9.92194e+00
41	6.26789e+00	7.71867e+05	1.34876e+06	5.18722e+00
42	7.53566e+00	0.00000e+00	4.44994e+04	2.24699e+00
43	9.05986e+00	0.00000e+00	6.33976e+02	1.29604e+00
44	1.08923e+01	0.00000e+00	3.49212e+00	7.46975e-01
45	1.30955e+01	0.00000e+00	6.12484e-03	8.43058e-01
46	1.57442e+01	0.00000e+00	2.66266e-06	2.43746e+00
47	1.89287e+01	0.00000e+00	2.44078e-10	1.50509e+00
48	2.27573e+01	0.00000e+00	3.13420e-15	9.01762e-01
49	2.73603e+01	0.00000e+00	3.80253e-21	5.38182e-01

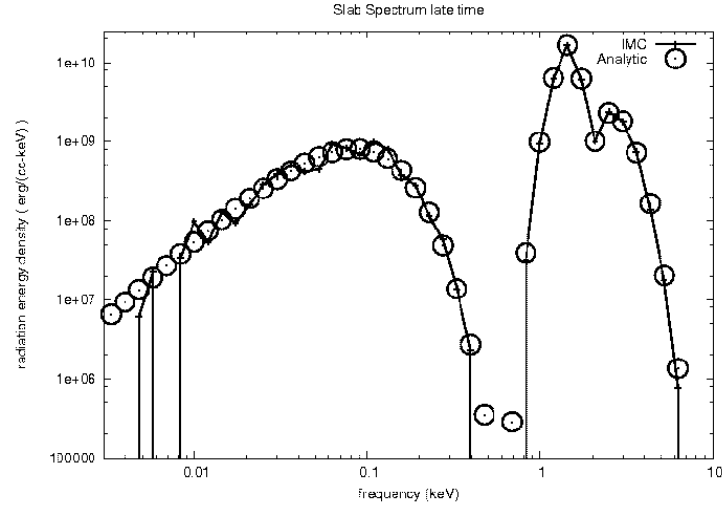


**Fig. 7.** The results for the slab version of the Graziani prompt spectrum problem and the analytic answer, Eqs. 21 and 23. Radiation energy density is plotted vs. frequency. Values of energy density at frequencies below .5 keV are from the thermal emission at  $T_c$  by the local matter. Values of energy density at frequencies above .5 keV are from higher frequency photons from the source, which have not been fully absorbed. These photons have frequencies at which the brominated plastic opacity has a small opacity and hence a large mean free path. (See Fig. 4.) The energy density is in units of  $\text{erg}/\text{cm}^3 - \text{keV}$  and the frequency is in units of keV.

## References

- [P73] G.C. Pomraning, *Equations of Radiation Hydrodynamics*, in International Series of Monographs in Natural Philosophy, edited by D. ter Harr (Pergamon, New York, 1973), Vol. 54.
- [BD77] W. E. Boyce and R. C. DiPrima, *Elementary Differential Equations and Boundary Value Problems*, 3rd edition, (John Wiley & Sons, New York, 1977)
- [FC71] Fleck, Jr., J. A., Cummings, J. D. : An Implicit Monte Carlo Scheme for Calculating time and frequency dependent nonlinear radiation transport. *J. Comp Phys.*, **31**, 313–342 (1971)
- [GKR98] Gentile, N. A., Keen, N., Rathkopf, J.: The KULL IMC Package, Tech. Rep. UCRL-JC-132743, Lawrence Livermore National Laboratory, Livermore CA (1998)
- [BM04] Brunner, T. A., Mehlhorn, T. A.: A User's Guide to Radiation Transport in ALEGRA-HEDPP, Tech. Rep. SAND-2004-5799, Sandia National Laboratories, Albuquerque, NM (2004)



- [G07] Graziani, F. : The Prompt Spectrum of a Radiating Sphere, Tech. Rep. UCRL-TR-232619-DRAFT, Lawrence Livermore National Laboratory, Livermore CA (2007)
- [CTh68] Cody, W., Thatcher, H: Rational Chebyshev Approximations for the Exponential Integral  $E_1(x)$ , Math. Comp., **22**, 641–649 (1968)
- [PTVF02] Press, W. Tuekolsky, S.A., Vetterling, W. T., Flannery, B. P.: *Numerical Recipes in C++*, Cambridge University Press, United Kingdom (2002)